HHS Public Access

Author manuscript

Cancer Lett. Author manuscript; available in PMC 2018 March 06.

Published in final edited form as:

Cancer Lett. 2014 February 01; 343(1): 14–23. doi:10.1016/j.canlet.2013.09.010.

Non-small cell lung cancer is susceptible to induction of DNA damage responses and inhibition of angiogenesis by telomere overhang oligonucleotides

Neelu Puri[a,*], **Ryan T. Pitman**[a], **Richard E. Mulnix**[a], **Terrianne Erickson**[a], **Audra N. Iness**[a], **Connie Vitali**[b], **Yutong Zhao**[c], and **Ravi Salgia**[d]

[a]Department of Biomedical Sciences, University of Illinois College of Medicine, Rockford, IL, United States

[b]Department of Pathology, University of Illinois College of Medicine, Rockford, IL, United States

[c]Department of Medicine, Division of Pulmonary, Allergy, Critical Care, University of Pittsburgh, Pittsburgh, PA, United States

[d]Department of Medicine, Section of Hematology/Oncology, University of Chicago, Chicago, IL, United States

Abstract

Exposure of the telomere overhang acts as a DNA damage signal, and exogenous administration of an 11-base oligonucleotide homologous to the 3′-telomere overhang sequence (T-oligo) mimics the effects of overhang exposure by inducing senescence and cell death in non-small cell lung cancer (NSCLC) cells, but not in normal bronchial epithelial cells. T-oligo-induced decrease in cellular proliferation in NSCLC is likely directed through both p53 and its homolog, p73, with subsequent induction of senescence and expression of senescence-associated proteins, p21, $p33^{ING}$, and $p27^{Kip1}$ both *in vivo* and *in vitro*. Additionally, T-oligo decreases tumor size and inhibits angiogenesis through decreased VEGF signaling and increased TSP-1 expression.

Keywords

Apoptosis; Lung cancer; Telomere overhang; Senescence; p53; Angiogenesis

1. Introduction

Lung cancer is notoriously difficult to treat with traditional chemotherapeutic options and recent advances in molecularly targeted therapies are plagued with difficulties including induced resistance and small therapeutically responsive populations [1]. There is a

*Corresponding author. Address: University of Illinois College of Medicine at Rockford, Department of Biomedical Sciences, 1601 Parkview Avenue, Rockford, IL 61107, United States. Tel.: +1 815 395 5678; fax: +1 815 395 5666. neelupur@uic.edu (N. Puri).

Conflict of Interest

The authors have no financial, personal or other conflicts that may or could inappropriately bias the work presented in this manuscript.

Appendix A. Supplementary material

Supplementary data associated with this article can be found, in the online version, at http://dx.doi.org/10.1016/j.canlet.2013.09.010.

considerable molecular heterogeneity in lung cancer, however, many lung cancers contain functional mutations in the important tumor suppressor p53, [2] which contributes to their malignancy and difficulty in treatment. At present, multiple treatment modalities are being pursued as new therapeutic options for lung cancer [1]. An interesting alternative strategy in lung cancer is targeting the telomere or telomerase, and recent strategies include small molecule or oligonucleotide inhibitors of telomerase [3–7] or an anti-telomerase vaccine [8]. We propose the use of an oligonucleotide homologous to the 3′ end of the human telomere as a potential therapeutic for lung cancer.

Telomeres are tandem repeats of a specific nucleotide sequence found at the end of chromosomes. The 3′ end of each telomere consists of a single stranded overhang of TTAGGG tandem repeats that has been proposed to stabilize a loop structure at the chromosome ends [9], and plays an important role in signaling for DNA damage responses. Acting like biological clocks, telomeres shorten with each successive round of DNA replication, and when critically short, signal for DNA damage responses resulting in cellular senescence or apoptosis [9]. In stem cells, telomeres are maintained by telomerase, an enzyme that extends the 3′ terminus of chromosome ends. Telomerase is generally not expressed in normal somatic cells, but is expressed in the majority of primary tumors and cancer derived cell lines [7]. The telomere overhang is protected by various telomere associated proteins, such as TRF2 and POT1 [9]. When these proteins are absent or nonfunctional, the telomere overhang is exposed, causing apoptosis, senescence, and differentiation [10].

We hypothesize the effects of telomere exposure can be artificially induced by exogenous addition of T-oligo, an 11-base oligonucleotide identical in sequence to the telomere overhang. T-oligo can induce DNA damage responses similar to those occurring under physiological conditions [11]. In fact, T-oligo, which accumulates in the nucleus [11], induces a DNA damage response in primary human cells including enhanced DNA repair [12], senescent phenotype in fibrosarcoma cells [13], and apoptosis in immortalized and malignant cell lines [11,14]. T-oligo responses are mediated in part through multiple DNA damage pathways including ATM kinases [15], p53 [11,12,14,15] or its homologue, p73 [11,14], p95/NBS1, E2F1, and pRb [13,15,16]. However, recent evidence suggests that ATM may not be as integral to T-oligo induced DNA damage responses as previously hypothesized [17]. T-oligo induced cellular responses occur without affecting the cells own telomeres [13,16,18] and are independent of telomerase [13]. Additional research into T-oligo's mechanism of action reveals that T-oligo may increase cellular reactive oxygen species levels through a p53 dependent pathway, indicating that T-oligo may also act to reduce oxidative damage to cells [18]. Thus, exposure to the telomere overhang sequence is able to target malignant cells through multiple p53 dependent and independent mechanisms.

Although the mechanism of a T-oligo induced DNA damage response remains unclear, an increasing number of malignant cell types display sensitivity to T-oligo in cell culture including breast, ovarian, prostate, pancreatic, melanoma, glioma, and lymphoma [14,17,19–23]. Particularly, T-oligo reduces tumorigenicity and metastasis of melanoma [14] and maintains *in vivo* efficacy against mouse models of breast cancer, glioma, and lymphoma [19,22,23] without toxic side effects on mice [9,14]. Remarkably, T-oligo has limited effects

on multiple normal cell types in comparison to their malignant counterparts [14,19,23]. The potency of T-oligo against cancer cell lines at relatively short treatment times and its lack of harmful effects on normal cells suggests its combination with other compounds may increase treatment efficacy without increasing cytotoxicity [9,14,24].

In addition to T-oligo's marked anti-tumor activity through induction of DNA damage responses, *in vitro* studies by Coleman et al. demonstrate that T-oligo may also reduce angiogenesis in melanoma by inhibiting DNA binding activity of the HIF-1 transcription factor contributing to decreased expression and release of the angiogenic factors, VEGF and ANG-1 [24]. However, no previous study demonstrates an effect of T-oligo on VEGF or TSP-1 expression *in vivo*. At present, experiments suggest that T-oligo is able to inhibit the growth of tumors through both classical DNA damage responses and inhibition of angiogenesis, however the mechanism of the latter has not yet been determined.

In this study, we examined the potential of T-oligo to induce senescence and decrease cellular proliferation in non-small cell lung cancer (NSCLC). We used the NSCLC cell lines SW1573 and H358, which have wild type p53 [25,26] and homozygous deletion of p53 [27–31], respectively, to determine if T-oligo could be useful in lung cancer with and without p53 expression. We further evaluated the use of T-oligo as a therapeutic treatment in NSCLC xenografts in nude mice and demonstrated both reduced tumor size and vascularity. Additionally, we validated T-oligo induced senescence *in vivo*, and demonstrated the importance of VEGF and TSP-1 in Toligo's effect on angiogenesis. With these studies we hope to demonstrate the efficacy of T-oligo in lung cancer and bring T-oligo closer to clinical use as a cancer therapeutic.

2. Materials and methods

2.1. Chemicals, cells, and antibodies

DNA oligonucleotides, homologous and complementary to the 3′ telomere overhang sequence (T-oligo: pGTTAGGGTTAG, and complementary oligonucleotide pCTAACCCTAAC, respectively) were obtained for cell culture and animal experiments from Midland Certified Reagent Company (Midland, TX). SW1573, H358, SK-LU-1, H226, SW900, and H1838 lung cancer cells were obtained from American Type Culture Collection (Rockville, MD), cultured according to the provided instructions, and used for experimentation at early passages. Basal media and balanced salt solutions were obtained from Gibco (Invitrogen, Carlsbad, CA). Normal bronchial epithelial cells (NBEC) were isolated from normal lung tissue using an established procedure [32] and maintained at 7% CO_2 and 37 °C in bronchial epithelial cell basal medium supplemented with gentamicin sulfate, transferrin, bovine pituitary extract, hydrocortisone, epidermal growth factor, insulin, epinephrine, triiodothyronine, and retinoic acid as per manufacturer's instructions (Lonza, MD). E2F1 antibodies were obtained from Santa Cruz Biotechnology, Inc. (Santa Cruz, CA). p53, p73 antibodies were purchased from EMD Millipore (Billerica, MA), and phospho-p53 (Ser 15) was purchased from Cell Signaling (Danvers, MA), Calcein AM was purchased from Invitrogen. Methylene blue was purchased from Bio-Rad Laboratories, Inc. (Hercules, CA). β-actin antibody, anti-mouse and anti-rabbit secondary antibodies, 5-

Bromo-4-chloro-3-indolyl β-D-galactopyranoside, propidium iodide, and all other chemicals were obtained from Sigma Aldrich (St. Louis, MO).

2.2. Inhibition of cell growth and determination of cell death

NBEC, SW1573, H1838, and H358 NSCLC cells were plated and treated with diluent (water), 40 μM T-oligo, or 40 μM complementary oligo for 48, 72, and 96 h. Cell proliferation was measured by counting the number of viable cells as determined by trypan blue exclusion subsequent to trypsinization [33]. Cell death was determined by propidium iodide staining and sub G_0/G_1 DNA analysis on a FACS scan (Becton Dickinson, Franklin Lakes, NJ) [14]. All experiments were performed in triplicate. Paired Student's *t*-test was used to evaluate the differences between T-oligo and complementary oligo groups. Significance was established at $\alpha = 0.05$.

2.3. Senescence and clonogenicity

Senescence in NBEC, SW1573 and H358 cells was determined by treating cells for one week with 40 μM T-oligo or 40 μM complementary oligo after which cells were fixed in 3.7% formaldehyde in phosphate buffered saline (PBS) for 5 min and washed twice with PBS. Cells were then stained with β-Galactosidase [16,34] for 16 h at 37 °C, and counterstained with Calcein AM [35]. Clonogenicity was studied by plating H358 and SW1573 cells at 25,000 cells/60 mm dish and treating with 40 μM T-oligo or 40 μM complementary oligo. After one week, cells were harvested with trypsin/EDTA and plated at 3000 cells/60 mm dish and incubated for eight days in growth medium. Cells were then fixed in 100% ethanol and stained with 1% methylene blue in PBS for 10 min [13]. Visible colonies were counted using Kodak ROI analysis. All experiments were performed in triplicate. Paired Student's *t*-test was used to evaluate the differences between T-oligo and complementary oligo groups. Significance was established at $\alpha = 0.05$.

2.4. Immunoblotting

H358 and SW1573 cells were treated with diluent, 40 μM complementary oligonucleotide, or 40 μM T-oligo for various time points after which protein expression was analyzed by immunoblotting [33]. Briefly, cells were washed twice with PBS and cell lysates were collected using 200 μL lysis buffer (20 mM Tris–HCl (pH 8.0), 150 mM NaCL, 100 mM NaF, 1% NP-40, 10% glycerol, 1 mM sodium orthovanadate, and 1× complete protease inhibitor; Roche Diagnostics, Indianapolis, IN). A sonicator was then used to homogenize cell lysates and protein concentration was determined by the Bio-Rad protein assay kit (Hercules, CA). 50 μg of protein from each sample was run on a SDS-PAGE gel and blots were probed with the aforementioned antibodies. Immunoblots were then visualized using Western Lightning ECL (Perkin Elmer, Waltham, MA). All experiments were performed in triplicate with similar outcomes.

2.5. Animals

Five-week old male *nu/nu* (nude) mice were purchased from Taconic (Hudson, NY), and housed in the pathogen-free animal facility at the University of Illinois, College of Medicine

at Rockford. All animal protocols were approved by the Institutional Biological Resource Committee from the University of Illinois, College of Medicine at Rockford.

2.6. NSCLC tumorigenicity

SW1573 and H358 cells were cultured as described above and harvested with trypsin/EDTA. Viability was determined by trypan blue exclusion. Only cell populations with ≥90% viability were used for this investigation. Cells were suspended in Hank's Balanced Salt Solution and 5×10^6 viable cells were injected subcutaneously into the flank or leg region of five-week old male *nu/nu* (nude) mice (Taconic, Hudson, NY) to establish tumors. After 72 h, mice were randomized and divided into two subgroups of 10. The T-oligo treatment group received daily intratumoral injections of 210 μg in 150 μl of PBS (60 nM) T-oligo and the control group received daily intratumoral injections of 210 μg of complementary oligonucleotide in 150 μl of PBS. Mice were weighed weekly and observed for signs of excessive tumor burden or toxicity. Weekly tumor measurements were performed by a blinded observer with digital calipers (Fisher Scientific, Hampton, NH). Tumor volume was calculated according to the formula: volume (mm^3) = (length × $width^2$)/2 [36]. After seven weeks, mice were euthanized and tumors were resected and preserved in either 4% formalin for subsequent paraffin embedding and immunohistochemical analysis or in OCT solution and flash frozen in an ethanol/ dry ice mixture and stored at −70 °C. Analysis of tumor growth was performed using paired Student's *t*-test to compare T-oligo and complementary oligo groups. Significance was established at $\alpha = 0.05$.

2.7. Senescence associated β-Galactosidase (SA-β-Gal) staining of tumor sections

Tumor sections were stained for SA-β-Gal as described previously [37]. Briefly, frozen tumors were sectioned into 4 μm slices using a cryostat (Damon/IEC minotome, Needham, MA). Tumor sections were placed on positively charged slides and fixed at 4 °C in 1% formalin in PBS for 1 min and washed thrice in 4 °C PBS. Sections were immersed in β-Galactosidase staining solution and incubated for 16 h at 37 °C. Sections were then fixed in 5% formalin for 10 min, washed twice with PBS at room temperature and counterstained with eosin. SA-β-Gal staining was performed on at least three separate tumors with similar results. For each experiment, the most representative tumor section was examined and photographed at 40× magnification.

2.8. Immunohistochemistry (IHC)

Paraffin sections of SW1573 and H358 tumors were prepared following standard immunohistochemical procedures. Briefly, sections were rehydrated using four successive decreasing concentrations of xylene and ethanol and then rinsed in PBS twice for 5 min. Antigen retrieval was performed by incubating rehydrated sections in a 0.05% trypsin, 1% calcium chloride solution for 10 min at 37 °C. Tumor sections were then stained using the M.O.M. IHC kit from Vector Labs (Burlingame, CA). Once desired staining intensity was obtained, slides were counterstained using hematoxylin (Sigma, St. Louis, MO) for 15 s, dehydrated in increasing concentrations of ethanol and xylene, and mounted with cover slip using Permount (Fisher, Rockford, IL). Photomicrographs were obtained with an Olympus BH-2 microscope (Olympus, Center Valley, PA) at 20× magnification. IHC was performed

on at least three separate tumors with similar results. For each experiment, the most representative tumor section was examined and photographed at 200× magnification.

2.9. Quantification of tumor microvessel quantity

H358 and SW1573 tumor sections were analyzed for microvessel density by immunohistochemistry for CD31, an endothelial cell specific marker. Vessels were counted at 200× magnification in at least 10 fields from three separate tumors by a blinded observer. Statistical analysis of tumor microvessel density was performed using paired Student's *t*-test to compare T-oligo and complementary oligo tumors. Significance was established at $\alpha = 0.05$. Photomicrographs were taken at 200× magnification from representative fields of tumors.

3. Results

3.1. Inhibition of cell growth and induction of cell death in lung cancer cell lines by exposure to oligonucleotides homologous to the telomere overhang

Previous studies demonstrate the potential for T-oligo, an 11-base oligonucleotide homologous to the telomere overhang, to inhibit the growth of multiple tumor types [14,17,19–23]. To determine T-oligo's efficacy in slowing the growth of lung cancer, we exposed six NSCLC cell lines (H1838, SK-LU-1, H358, H226, SW900, SW1573) to T-oligo, or an oligonucleotide complementary to the telomere overhang. Cells exposed to T-oligo exhibit a 40– 50% inhibition of growth as compared to the complementary oligo (Fig. 1A) with maximal inhibition of H1838 cell growth (Fig. 1A). We have made a titration curve with increasing concentrations of T-oligo ranging from 10 μM to 100 μM in p53 wild-type SW1573 and p53 null H358 cell lines (Supplementary Fig. 1S). T-oligo inhibited cell growth in both cell lines comparably, H358 from 28% to 85% and SW 1573 from 22% to 82% compared to complementary oligonucleotide. This level of growth inhibition is comparable with other cancers like melanoma, prostate and glioma [14,21,22].

Further analysis of T-oligo treated H1838 and H358 cells demonstrate a 3-fold and 4-fold increase in cell death via propidium iodide staining and FACS analysis as compared to complementary oligonucleotide, respectively (Fig. 1B and C). T-oligo also induces activation of caspase 9 and 3 after 12 and 24 h in H1838 cells, respectively (Fig. 1D). These results demonstrate T-oligo's powerful ability to inhibit cell growth in a wide-range of NSCLC cell types and suggest that caspase-mediated cell death may be one of the mechanisms for T-oligo's anti-tumor effect.

3.2. Increased p53 and p73 after exposure to telomere overhang oligonucleotides in NSCLC cells

Our evidence demonstrates that exposure to the telomere overhang DNA sequence induces a potent apoptotic response in NSCLC cells similar to T-oligo-induced DNA damage responses observed in multiple other malignant cells [14,19,21]. Previous reports in our lab and others suggest that the T-oligo induced DNA damage response is mediated, at least in-part, through the tumor suppressor p53 [9]. However, p53 is either silenced or inactivated in many NSCLC cell types [2]. To determine the potential for p53 dependent and independent

telomere overhang induced DNA damage responses in NSCLC cells, we studied NSCLC cells expressing both wild-type p53 (SW1573) [25,26] or with a homozygous deletion of p53(H358), but expressing wild-type p73, a p53 homologue [30,31]. As described above, both H358 and SW1573 exhibit a significant decrease in cell viability after exposure to T-oligo (Fig. 1A). In SW1573 cells, T-oligo treatment induces significant upregulation and phosphorylation of p53 (Ser15) after 12 h (Fig. 2A). In addition, E2F1, a downstream co-transcriptional factor of p53 [38], and p21, a downstream transcriptional product of activated p53 [39], are upregulated at 24 h in SW1573 cells (Fig. 2B). Interestingly, in p53-deficient H358 cells, p73 is upregulated at 12 h (Fig. 2C). Previous results suggest the importance of both p53 [13] and p73 [11,14] in T-oligo induced apoptosis, and our results confirm that they play a similarly important role in NSCLC. Furthermore, decreased cellular proliferation coupled to increased expression of p73 in H358 suggests that T-oligo may be effective in NSCLC tumors that lack functional p53 and contain functional p73.

3.3. SW1573 and H358 NSCLC cells are susceptible to T-oligo induced senescence

In addition to apoptosis, replicative senescence is a well-defined mechanism of tumor suppression, previously shown to be induced by oligonucleotides homologous to the telomere overhang [13,16]. Additionally, previous results demonstrate induction of senescence *in vitro* by T-oligo in other cancers [13,19,40]. However, no study has determined if exposure to the telomere overhang sequence can induce senescence in NSCLC cells. Both H358 (Fig. 3A) and SW1573 (Fig. 3C) cells exhibit altered morphology and an increase in size similar to that of senescent fibroblasts [16] after exposure to T-oligo for one week, suggesting that exposure of the telomere overhang may induce a senescent phenotype in malignant NSCLC cells. Furthermore, H358 cells treated with T-oligo demonstrate a 12-fold increase in number of cells positive for the presence of SA-β-Gal, a senescence specific marker (Fig. 3A) [34], while a 4-fold increase is observed in SW1573 cells (Fig. 3C) in comparison to cells treated with a complementary oligonucleotide. To further establish a T-oligo induced senescent state [41], the clonogenic capacity of H358 and SW1573 cells was determined by treating the cells with T-oligo for one week, reseeding and culturing for two additional weeks, and subsequently staining with methylene blue. Clonogenic capacity is decreased in both H358 (Fig. 3B) and SW1573 cells (Fig. 3D) by 12-fold and 4-fold, respectively, in comparison to complementary oligonucleotide treated cells. These results demonstrate that exposure to the telomere overhang sequence induces senescence in both wild-type p53 (SW1573) and p53 deficient (H358) NSCLC cells, and suggests a role for T-oligo induced senescence in both.

3.4. Normal bronchial cells are not susceptible to T-oligo-induced activation of DNA damage response pathway

We show that T-oligo induces a significant decrease in NSCLC proliferation, likely through p53 and p73 induced cell death and senescence. For that reason, we investigated the ability of T-oligo to induce cell death or senescence in normal bronchial epithelial cells (NBEC). Non-malignant NBEC treated with T-oligo in a manner identical to NSCLC cells did not exhibit significant differences in cell proliferation at 72 or 96 h (Fig. 4A), and FACS analysis after propidium iodide staining indicates no induction of cellular death after treatment with T-oligo (Fig. 4B). In addition, NBEC exposed to T-oligo and stained with SA-β-Gal showed

negligible induction of senescence (Fig. 4C). Accordingly, exposure to T-oligo caused no increase in p53 or p21 expression at 12 or 24 h in NBEC as seen by immunoblotting (Fig. 4D). These results indicate that T-oligo's anti-tumor effects are specific for cancerous NSCLC with minimal or no effect on normal lung tissues.

3.5. T-oligo reduces tumorigenicity and induces senescence in NSCLC tumor xenografts

While T-oligo inhibits melanoma tumor growth and decreases metastatic potential [14], the efficacy of T-oligo treatment in NSCLC *in vivo* is unknown. SW1573 and H358 tumors were formed in the flanks of *nu/nu* (nude) mice and treated with daily intratumoral injections of T-oligo or complementary oligo for seven weeks. T-oligo significantly reduced tumor size of both H358 and SW1573 tumors by 80% ($p < 0.0001$) and 88% ($p<0.001$), respectively (Fig. 5A and B). Further analysis of tumor tissue by SA-β-Gal staining indicates that T-oligo, but not complementary oligo, induces senescence *in vivo*. H358 tumors stained strongly for senescence associated-β-Galactosidase (Fig. 5C) while SW1573 tumors demonstrated less intense staining (Fig. 5D). These *in vivo* results are the first to demonstrate T-oligo induced senescence *in vivo* and are in concordance with our *in vitro* results.

3.6. T-oligo induced senescence in associated proteins in vitro and in vivo

To further evaluate T-oligo induced senescence in NSCLC, we immunoblotted SW1573 and H358 cells for the senescence-inducing proteins p33, $p27^{kip1}$, pRb, p16 and p21 [16,42,43]. T-oligo treated H358 cells demonstrated upregulation of p33 at both 48 h (2.2-fold) and 96 h (1.6-fold). Upregulation of p27 (1.8-fold), pRb (3-fold), p16 (2-fold) and p21 (2-fold) were also seen after 48 h (Fig. 6A). In p16 mutantSW1573 [44] cells upregulation of p33 (2-fold) at 96 h, $p27^{kip1}$ (1.8-fold) and p21 (2-fold) at 72 h are seen (Fig. 6B). Further, SW1573 tumors treated as described above demonstrate marked upregulation of p33, p21, and p27 as compared to tumor xenografts treated with complementary oligonucleotide (Fig. 6C) with similar results observed in H358 tumors (data not shown). Although upregulation of p33, p21 and $p27^{kip1}$ has been reported after exposure to telomere oligonucleotides *in vitro* [16], our results are the first to demonstrate the induction of these proteins *in vivo*, and further support the notion that senescence is a major contributor to T-oligo's anti-tumor effects.

3.7. NSCLC angiogenesis is inhibited by T-oligo through a decrease in VEGF and TSP-1

Since Coleman et al. demonstrate that MM-AN melanoma xenografts experience reduced angiogenesis in response to T-oligo treatment [24], we determined the susceptibility of NSCLC xenografts to inhibition of angiogenesis by T-oligo. Tumors were prepared as described above and immunostained for the presence of CD31, a marker specific to endothelial cells [45] (Fig. 7A), and VEGF, a marker of vessel density in lung cancer [46]. Vessel density in T-oligo treated H358 and SW1573 tumors, determined by counting vessels stained with CD31, decreased by 2.2-fold and 3-fold, respectively, compared to complementary oligonucleotide (Fig. 7B). A corresponding decrease in VEGF staining intensity is seen in both H358 and SW1573 tumors after treatment with T-oligo (Fig. 7C). To further explore the regulation of VEGF by T-oligo, we also stained tumor sections with TSP-1, an angiogenesis inhibitor with negative modulation of VEGF signaling [47]. As expected, TSP-1 staining intensity was markedly increased by exposure to Toligo (Fig. 7D).

These results confirm T-oligo's inhibition of angiogenesis seen in melanoma, and establish TSP-1 as a potential mediator of T-oligo's effect on VEGF and angiogenesis.

4. Discussion

In this study, we demonstrate that an 11-base oligonucleotide homologous to the 3′ telomere overhang prevents proliferation through induction of cell death and/or senescence in H358, H1838 and SW1573 NSCLC cell lines. Furthermore, we demonstrate a similar induction of senescence and inhibition of angiogenesis in NSCLC xenografts in nude mice, supporting the development of T-oligo as a therapeutic modality [14]. Importantly, T-oligo has no observed deleterious effects in NBEC.

DNA damage responses are proposed to mediate the anti-cancer effects of T-oligo through activation of multiple independent DNA damage pathways including p53, p95/Nbs1, E2F1, and $p16^{INK4A}$ [13–16]. Our results show that administration of T-oligo decreases cellular proliferation in all NSCLC cell lines with evidence for activation of the DNA damage responses in SW1573 and H358 cells. Upregulation and phosphorylation of p73 or p53 is likely to drive cell death through activation of caspase 9 and 3 in H1838 cells and p21 in SW1573 [23]. Recent studies have demonstrated that T-oligo can induce apoptosis in a p53 independent manner using either cdk2 or extrinsic apoptotic pathways through TRAIL death-receptor signaling by the activation of JNK which activates caspases 8 and 3 [17,48]. However, our studies indicate activation of caspase 9 and 3 suggesting the involvement of an intrinsic pathway which may be mediated by p53 or p73. These results corroborate previous findings including recent results which demonstrate a 40% reduction in apoptosis after siRNA mediated knockdown of p53 in p53-expressing MU melanoma cells [11,49] and suggest an important role for DNA damage responses mediated through a p53-dependent pathway.

The p53 homologue p73 is also implicated in T-oligo induced DNA damage responses as p53 deficient H358 cells that express wild-type p73 also undergo significant cell death and senescence. Moreover, expression of a dominant negative p73 in p53 deficient MM-AN melanoma cells decreases T-oligo induced apoptosis by 50% [11]. Our results substantiate prior findings and confirm a p73 or p53-dependent mechanism of T-oligo induced DNA damage response in NSCLC. The apoptotic response downstream to the DNA damage response induced by T-oligo is well described in many tumor types including melanoma, pancreatic, breast and prostate [14,17,19,21]. In the present study, T-oligo decreases cellular proliferation in all NSCLC cell lines and cell death that may be attributable to apoptosis is documented in both H1838 and H358 cells. These results confirm the vital role of apoptosis/cell death in T-oligo's potential therapeutic effect which has also been observed by earlier investigators [9,14,19].

Senescence is a vital modality for prevention and treatment of cancer [50]. In conjunction with clonogenic capacity, it is considered a reliable marker for predicting cancer treatment response [50,51]. Senescence has previously been demonstrated as an important pathway of the DNA damage response elicited by exposure to T-oligo in cultured fibrosarcoma [13] and MCF-7 breast cancer cells [19], and we demonstrate potent induction of senescence in

NSCLC cells after exposure to T-oligo (Fig. 3A and C). Previous evidence shows that T-oligo induced senescent cells exhibit p53 activation in addition to induction and upregulation of the cyclin-dependent kinase inhibitors, p21 and p16, and subsequent reduction in Rb phosphorylation [16]. Unfortunately, many tumors contain functional mutations of p53 [2], however, the ability for Toligo to induce senescence in the absence of p53 is currently not defined. In the present study we observed upregulation of p16, an important senescent marker, in our p53 null cell line suggesting its role in T-oligo mediated senescence along with p73 [16]. Interestingly, p53 deficient H358 cells exhibit a greater senescent response to T-oligo which may suggest a preference for induction of senescence through p73 and/or p16 in the absence of p53 after T-oligo exposure [52].

Senescence is mediated in part through the activation of specific DNA damage responsive proteins including $p27^{kip1}$, p33, and p21. p21 is upregulated by p53 signaling and functions by inhibiting CDK2, and through inhibition of the catalytic capacity of CDK4, preventing CDK4 from phosphorylating Rb and causing cell cycle arrest in the G_1 phase [39]. $p27^{kip1}$ functions downstream of both p21 and pRb and functions by inhibiting the catalytic capacity of CDK2 with subsequent cell cycle arrest in the G_1 phase, while p33 co-precipitates with p53 and enhances transactivation of p21 leading to cell cycle arrest and senescence [42]. Immunoblotting of H358 and SW1573 cell lysates and SW1573 tumors confirms the role of p21, p33, and $p27^{kip1}$ in T-oligo mediated senescence in NSCLC both *in vitro* and *in vivo*. Our results confirm previous findings [16], and further our knowledge of T-oligo's therapeutic potential in the absence of functional p53, as no previous study has verified senescence in cell lines without functional p53. Thus, our results indicate that T-oligo could be effective against lung cancer by mediating senescence in the presence and absence of p53.

Apoptosis is induced by p53 and its homologue p73 through transcriptional activation of BAX [53,54], which leads to release of cytochrome c and activation of caspases. These are rapid sequential events, with caspase activation occurring in as little as 12 h in H1838 cells. However, T-oligo induced senescence is a slower and a multiple step process involving p53/p21 and p16/ pRb and modulation of their downstream target proteins which may take several days to induce senescence [16,19]. Our studies demonstrate that both p53 and p73 can mediate T-oligo induced senescence and also substantiate the role of p73, which has been earlier shown to induce senescence in cancer cells [55,56]. Thus, it is entirely possible for p53 or p73 to drive the induction of both cell death and senescence with variable time courses.

Due to the many deleterious side effects associated with both chemotherapeutics and modern molecularly targeted therapies [57,58], we wanted to determine if exposure to T-oligo might also decrease the cell viability of normal bronchial cells. It was found that treatment of non-malignant NBEC with T-oligo does not decrease cell proliferation, induce cell death or senescence, or increase the expression of proteins associated with DNA damage response pathways, p53 or p21 (Fig. 4). These findings demonstrate that T-oligo has no negative effects on NBEC, and are encouraging as T-oligo could prove to be a useful new therapeutic agent. These results validate other studies by Longe et al., Yaar et al. and Puri et al. which showed that T-oligo has minimal or no DNA damage response in normal primary peripheral

blood leukocytes, normal mammary cells, and normal human melanocytes [14,19,23]. Unlike previous studies where T-oligo-exposed normal human melanocytes underwent S-phase arrest [14], and normal mammary cells exposed to T-oligo had decreased cellular proliferation and increased expression of phospho-p53^{Ser15} [19], to our knowledge this is the first study which demonstrates that T-oligo has no observable deleterious effect on the corresponding normal NBEC. These findings suggest that T-oligo may have the ability to spare normal cells from cytotoxic effects, while inducing senescence and cell death in cancer cells, and supports the development of T-oligo as a potential cancer therapeutic with very few side effects.

This study establishes the susceptibility of NSCLC to DNA damage responses *in vitro* without demonstration of deleterious effects in NBEC. To extend these results and further suggest the therapeutic potential of T-oligo in NSCLC, we demonstrate reduced NSCLC tumor volume and induction of senescence in H358 and SW1573 tumors in nude mice (Fig. 5). Interestingly, the effect of T-oligo on H358 tumors was more significant than T-oligo's effect on SW1573 tumors, which may be attributed to the lack of p53 in H358 cells or a preference for senescence upon exposure to T-oligo in H358 tumors by p73. Of note, tumors with mutated or absent p53 are often resistant to chemotherapy [59], thus increased susceptibility of H358 to T-oligo may indicate a new method to target p53 deficient NSCLC. In addition to the enhanced susceptibility of p53 deficient H358 tumors to T-oligo, we are the first, to our knowledge, to demonstrate induction of senescence by T-oligo *in vivo*. Previous studies also demonstrate a therapeutic potential for T-oligo as intratumoral and intravenous T-oligo treatment decreases melanoma tumor growth, and pretreatment with T-oligo decreases the metastatic potential of melanoma cells [14,24]. Further, intravenous T-oligo increases survival time in MCF-7 metastatic breast tumor model [19] and prolongs survival time and decreases tumor size in a model of glial tumors [22]. These results confirm our *in vitro* findings and, coupled with the findings of others, suggest that future work on T-oligo should be focused on increasing the clinical relevance of this telomere oligonucleotide as a novel cancer therapeutic.

Coleman et al. demonstrate a reduction of tumor microvascular density and functional vessels density by 80% after intravenous treatment with T-oligo [24]. In our study, we demonstrate a 92% decrease in angiogenesis in SW1573 coupled with decreased expression of VEGF and increased expression of TSP-1 *in vivo* in both p53 wild-type (SW1573) and p53 deficient (H358) cells (Fig. 7). To our knowledge, this is the first documentation of alterations in TSP-1 expression in response to exposure to the telomere overhang sequence. These results are novel and highlight a new direction in telomere-based therapeutics research. However, the mechanism of T-oligo's effect on angiogenesis is unclear. Typically, HIF-1α and VEGF work concurrently to drive angiogenesis in response to hypoxia [60], however, this pathway can be inhibited, both directly and indirectly, by p53 in response to DNA damage [61]. Furthermore, TSP-1, a negative modulator of VEGF expression, may be regulated by p53 [62], suggesting a potential role for the T-oligo-induced DNA damage response on the inhibition of angiogenesis. Unfortunately, the role of p73 in the inhibition of angiogenesis is presently unclear as p73 overexpression inhibits VEGF expression in lymphoma cells [63] while promoting VEGF expression and reducing TSP-1 expression in ovarian carcinoma cells [64]. Our results, in conjunction with others demonstrate a potential

role for p73 in T-oligo induced reduction in angiogenesis as both H358 and MM-AN, which are deficient in p53 and display marked decrease in angiogenesis in response to T-oligo [24]. E2F1, in addition to acting as a driver of p53- and p73-induced apoptosis, is a transcription factor that directly regulates TSP-1 expression [65], and is known to be induced by T-oligo exposure [11,14,24]. In light of this data, we suggest further analysis of the role of E2F1 in T-oligo's reduction in angiogenesis.

5. Concluding remarks and future directions

This study extends the feasibility of the use of oligonucleotides homologous to the 3′-telomere overhang as cancer therapeutics specific for malignant cells, and exemplifies the multiple pathways utilized by the telomere overhang sequence to prevent cancer growth. The disparity in response between malignant cells and normal cells suggests the possibility of an alteration in the DNA damage response pathway in malignant cells that is exploited by T-oligo. Further research may identify and make use of this altered DNA damage response as a pharmacological method of targeting malignant cells specifically.

Supplementary Material

Refer to Web version on PubMed Central for supplementary material.

Acknowledgments

We would like to acknowledge Deven Etnyre and Jason Fong for their technical assistance and for their assistance in preparation of the manuscript. This research was funded through pilot grant funding obtained through the University of Illinois at Chicago Cancer Center to Neelu Puri.

References

1. Salgia R, Hensing T, Campbell N, Salama AK, Maitland M, Hoffman P, Villaflor V, Vokes EE. Personalized treatment of lung cancer. Semin. Oncol. 2011; 38:274–283. [PubMed: 21421117]
2. Campling BG, el-Deiry WS. Clinical implications of p53 mutations in lung cancer. Methods Mol. Med. 2003; 75:53–77. [PubMed: 12407735]
3. Kim MY, Vankayalapati H, Shin-Ya K, Wierzba K, Hurley LH. Telomestatin, a potent telomerase inhibitor that interacts quite specifically with the human telomeric intramolecular g-quadruplex. J. Am. Chem. Soc. 2002; 124:2098–2099. [PubMed: 11878947]
4. Gowan SM, Heald R, Stevens MF, Kelland LR. Potent inhibition of telomerase by small-molecule pentacyclic acridines capable of interacting with G-quadruplexes. Mol. Pharmacol. 2001; 60:981–988. [PubMed: 11641426]
5. Gowan SM, Harrison JR, Patterson L, Valenti M, Read MA, Neidle S, Kelland LR. A G-quadruplex-interactive potent small-molecule inhibitor of telomerase exhibiting in vitro and in vivo antitumor activity. Mol. Pharmacol. 2002; 61:1154–1162. [PubMed: 11961134]
6. Dikmen ZG, Wright WE, Shay JW, Gryaznov SM. Telomerase targeted oligonucleotide thio-phosphoramidates in T24-luc bladder cancer cells. J. Cell. Biochem. 2008; 104:444–452. [PubMed: 18044713]
7. Ruden M, Puri N. Novel anticancer therapeutics targeting telomerase. Cancer Treat. Rev. 2013; 39:444–456. [PubMed: 22841437]
8. Brower V. Telomerase-based therapies emerging slowly. J. Natl. Cancer Inst. 2010; 102:520–521. [PubMed: 20388877]

9. Rankin AM, Faller DV, Spanjaard RA. Telomerase inhibitors and 'T-oligo' as cancer therapeutics: contrasting molecular mechanisms of cytotoxicity. Anticancer Drugs. 2008; 19:329–338. [PubMed: 18454043]
10. Karlseder J, Broccoli D, Dai Y, Hardy S, de Lange T. P53- and ATM-dependent apoptosis induced by telomeres lacking TRF2. Science. 1999; 283:1321–1325. [PubMed: 10037601]
11. Eller MS, Puri N, Hadshiew IM, Venna SS, Gilchrest BA. Induction of apoptosis by telomere 3′ overhang-specific DNA. Exp. Cell Res. 2002; 276:185–193. [PubMed: 12027448]
12. Eller MS, Maeda T, Magnoni C, Atwal D, Gilchrest BA. Enhancement of DNA repair in human skin cells by thymidine dinucleotides: evidence for a p53- mediated mammalian SOS response. Proc. Natl. Acad. Sci. USA. 1997; 94:12627–12632. [PubMed: 9356500]
13. Li GZ, Eller MS, Hanna K, Gilchrest BA. Signaling pathway requirements for induction of senescence by telomere homolog oligonucleotides. Exp. Cell Res. 2004; 301:189–200. [PubMed: 15530855]
14. Puri N, Eller MS, Byers HR, Dykstra S, Kubera J, Gilchrest BA. Telomere-based DNA damage responses: a new approach to melanoma. Faseb J. 2004; 18:1373–1381. [PubMed: 15333580]
15. Eller MS, Li GZ, Firoozabadi R, Puri N, Gilchrest BA. Induction of a p95/Nbs1-mediated S phase checkpoint by telomere 3′ overhang specific DNA. Faseb J. 2003; 17:152–162. [PubMed: 12554694]
16. Li GZ, Eller MS, Firoozabadi R, Gilchrest BA. Evidence that exposure of the telomere 3′ overhang sequence induces senescence. Proc. Natl. Acad. Sci. USA. 2003; 100:527–531. [PubMed: 12515865]
17. Rankin AM, Sarkar S, Faller DV. Mechanism of T-oligo-induced cell cycle arrest in Mia-PaCa pancreatic cancer cells. J. Cell. Physiol. 2012; 227:2586–2594. [PubMed: 21898405]
18. Lee MS, Yaar M, Eller MS, Runger TM, Gao Y, Gilchrest BA. Telomeric DNA induces p53-dependent reactive oxygen species and protects against oxidative damage. J. Dermatol. Sci. 2009; 56:154–162. [PubMed: 19906512]
19. Yaar M, Eller MS, Panova I, Kubera J, Wee LH, Cowan KH, Gilchrest BA. Telomeric DNA induces apoptosis and senescence of human breast carcinoma cells. Breast Cancer Res. 2007; 9:R13. [PubMed: 17257427]
20. Sarkar S, Faller DV. T-oligos inhibit growth and induce apoptosis in human ovarian cancer cells. Oligonucleotides. 2011; 21:47–53. [PubMed: 21281128]
21. Gnanasekar M, Thirugnanam S, Zheng G, Chen A, Ramaswamy K. T-oligo induces apoptosis in advanced prostate cancer cells. Oligonucleotides. 2009; 19:287–292. [PubMed: 19642913]
22. Aoki H, Iwado E, Eller MS, Kondo Y, Fujiwara K, Li GZ, Hess KR, Siwak DR, Sawaya R, Mills GB, Gilchrest BA, Kondo S. Telomere 3′ overhang-specific DNA oligonucleotides induce autophagy in malignant glioma cells. Faseb J. 2007; 21:2918–2930. [PubMed: 17449721]
23. Longe HO, Romesser PB, Rankin AM, Faller DV, Eller MS, Gilchrest BA, Denis GV. Telomere homolog oligonucleotides induce apoptosis in malignant but not in normal lymphoid cells: mechanism and therapeutic potential. Int. J. Cancer. 2009; 124:473–482. [PubMed: 19003960]
24. Coleman C, Levine D, Kishore R, Qin G, Thorne T, Lambers E, Sasi SP, Yaar M, Gilchrest BA, Goukassian DA. Inhibition of melanoma angiogenesis by telomere homolog oligonucleotides. J. Oncol. 2010; 2010:928628. [PubMed: 20652008]
25. Jiang H, Reinhardt HC, Bartkova J, Tommiska J, Blomqvist C, Nevanlinna H, Bartek J, Yaffe MB, Hemann MT. The combined status of ATM and p53 link tumor development with therapeutic response. Genes Dev. 2009; 23:1895–1909. [PubMed: 19608766]
26. Oliver TG, Meylan E, Chang GP, Xue W, Burke JR, Humpton TJ, Hubbard D, Bhutkar A, Jacks T. Caspase-2-mediated cleavage of Mdm2 creates a p53-induced positive feedback loop. Mol. Cell. 2010; 43:57–71.
27. Shao C, Lu C, Chen L, Koty PP, Cobos E, Gao W. P53-Dependent anticancer effects of leptomycin B on lung adenocarcinoma, Cancer Chemother. Pharmacol. 2011; 67:1369–1380.
28. Ling YH, Liebes L, Jiang JD, Holland JF, Elliott PJ, Adams J, Muggia FM, Perez-Soler R. Mechanisms of proteasome inhibitor PS-341-induced G(2)-M-phase arrest and apoptosis in human non-small cell lung cancer cell lines. Clin. Cancer Res. 2003; 9:1145–1154. [PubMed: 12631620]

29. Dubrez L, Coll JL, Hurbin A, de Fraipont F, Lantejoul S, Favrot MC. Cell cycle arrest is sufficient for p53-mediated tumor regression. Gene Ther. 2001; 8:1705–1712. [PubMed: 11892838]
30. Courtois S, Caron de Fromentel C, Hainaut P. P53 protein variants: structural and functional similarities with p63 and p73 isoforms. Oncogene. 2004; 23:631–638. [PubMed: 14737098]
31. Takahashi T, Carbone D, Nau MM, Hida T, Linnoila I, Ueda R, Minna JD. Wild-type but not mutant p53 suppresses the growth of human lung cancer cells bearing multiple genetic lesions. Cancer Res. 1992; 52:2340–2343. [PubMed: 1559236]
32. Zhao Y, He D, Saatian B, Watkins T, Spannhake EW, Pyne NJ, Natarajan V. Regulation of lysophosphatidic acid-induced epidermal growth factor receptor transactivation and interleukin-8 secretion in human bronchial epithelial cells by protein kinase Cdelta Lyn kinase, and matrix metalloproteinases. J. Biol. Chem. 2006; 281:19501–19511. [PubMed: 16687414]
33. Puri N, Salgia R. Synergism of EGFR and c-Met pathways, cross-talk and inhibition, in non-small cell lung cancer. J. Carcinog. 2008; 7:9. [PubMed: 19240370]
34. Itahana K, Campisi J, Dimri GP. Methods to detect biomarkers of cellular senescence: the senescence-associated beta-galactosidase assay. Methods Mol. Biol. 2007; 371:21–31. [PubMed: 17634571]
35. Pao W, Miller VA, Politi KA, Riely GJ, Somwar R, Zakowski MF, Kris MG, Varmus H. Acquired resistance of lung adenocarcinomas to gefitinib or erlotinib is associated with a second mutation in the EGFR kinase domain. PLoS Med. 2005; 2:e73. [PubMed: 15737014]
36. Su F, Kozak KR, Imaizumi S, Gao F, Amneus MW, Grijalva V, Ng C, Wagner A, Hough G, Farias-Eisner G, Anantharamaiah GM, Van Lenten BJ, Navab M, Fogelman AM, Reddy ST, Farias-Eisner R. Apolipoprotein A-I (apoA-I) and apoA-I mimetic peptides inhibit tumor development in a mouse model of ovarian cancer. Proc. Natl. Acad. Sci. USA. 2010; 107:19997–20002. [PubMed: 21041624]
37. Dimri GP, Lee X, Basile G, Acosta M, Scott G, Roskelley C, Medrano EE, Linskens M, Rubelj I, Pereira-Smith O, et al. A biomarker that identifies senescent human cells in culture and in aging skin in vivo. Proc. Natl. Acad. Sci. USA. 1995; 92:9363–9367. [PubMed: 7568133]
38. Kowalik TF, DeGregori J, Leone G, Jakoi L, Nevins JR. E2F1-specific induction of apoptosis and p53 accumulation, which is blocked by Mdm2. Cell Growth Differ. 1998; 9:113–118. [PubMed: 9486847]
39. He G, Siddik ZH, Huang Z, Wang R, Koomen J, Kobayashi R, Khokhar AR, Kuang J. Induction of p21 by p53 following DNA damage inhibits both Cdk4 and Cdk2 activities. Oncogene. 2005; 24:2929–2943. [PubMed: 15735718]
40. Weng D, Cunin MC, Song B, Price BD, Eller MS, Gilchrest BA, Calderwood SK, Gong J. Radiosensitization of mammary carcinoma cells by telomere homolog oligonucleotide pretreatment. Breast Cancer Res. 2010; 12:R71. [PubMed: 20846433]
41. Chang BD, Broude EV, Dokmanovic M, Zhu H, Ruth A, Xuan Y, Kandel ES, Lausch E, Christov K, Roninson IB. A senescence-like phenotype distinguishes tumor cells that undergo terminal proliferation arrest after exposure to anticancer agents. Cancer Res. 1999; 59:3761–3767. [PubMed: 10446993]
42. Garkavtsev I, Grigorian IA, Ossovskaya VS, Chernov MV, Chumakov PM, Gudkov AV. The candidate tumour suppressor p33ING1 cooperates with p53 in cell growth control. Nature. 1998; 391:295–298. [PubMed: 9440695]
43. He G, Kuang J, Huang Z, Koomen J, Kobayashi R, Khokhar AR, Siddik ZH. Upregulation of p27 and its inhibition of CDK2/cyclin E activity following DNA damage by a novel platinum agent are dependent on the expression of p21. Br. J. Cancer. 2006; 95:1514–1524. [PubMed: 17088910]
44. Bamford S, Dawson E, Forbes S, Clements J, Pettett R, Dogan A, Flanagan A, Teague J, Futreal PA, Stratton MR, Wooster R. The COSMIC (Catalogue of Somatic Mutations in Cancer) database and website. Br. J. Cancer. 2004; 91:355–358. [PubMed: 15188009]
45. Wang D, Stockard CR, Harkins L, Lott P, Salih C, Yuan K, Buchsbaum D, Hashim A, Zayzafoon M, Hardy RW, Hameed O, Grizzle W, Siegal GP. Immunohistochemistry in the evaluation of neovascularization in tumor xenografts. Biotechnol. Histochem. 2008; 83:179–189.
46. Lund EL, Thorsen C, Pedersen MW, Junker N, Kristjansen PE. Relationship between vessel density and expression of vascular endothelial growth factor and basic fibroblast growth factor in

small cell lung cancer in vivo and in vitro. Clin. Cancer Res. 2000; 6:4287–4291. [PubMed: 11106245]

47. Lawler PR, Lawler J. Molecular basis for the regulation of angiogenesis by thrombospondin-1 and-2. Cold Spring Harbor Perspect. Med. 2012; 2:a006627.
48. Sarkar S, Faller DV. Telomere-homologous G-rich oligonucleotides sensitize human ovarian cancer cells to TRAIL-induced growth inhibition and apoptosis. Nucleic Acid Ther. 2013; 23:167–174. [PubMed: 23634944]
49. Pitman RT, Wojdyla L, Puri N. Mechanism of DNA damage responses induced by exposure to an oligonucleotide homologous to the telomere overhang in melanoma. Oncotarget. 2013; 4:761–771. [PubMed: 23800953]
50. Roninson IB, Broude EV, Chang BD. If not apoptosis, then what? Treatment-induced senescence and mitotic catastrophe in tumor cells. Drug Resist Updat. 2001; 4:303–313. [PubMed: 11991684]
51. Brown JM, Wouters BG. Apoptosis, p53, and tumor cell sensitivity to anticancer agents. Cancer Res. 1999; 59:1391–1399. [PubMed: 10197600]
52. Fang L, Lee SW, Aaronson SA. Comparative analysis of p73 and p53 regulation and effector functions. J. Cell Biol. 1999; 147:823–830. [PubMed: 10562283]
53. Polager S, Ginsberg D. P53 and E2f: partners in life and death. Nat. Rev. Cancer. 2009; 9:738–748. [PubMed: 19776743]
54. Melino G, Bernassola F, Ranalli M, Yee K, Zong WX, Corazzari M, Knight RA, Green DR, Thompson C, Vousden KH. P73 Induces apoptosis via PUMA transactivation and Bax mitochondrial translocation. J. Biol. Chem. 2004; 279:8076–8083. [PubMed: 14634023]
55. Jung MS, Yun J, Chae HD, Kim JM, Kim SC, Choi TS, Shin DY. P53 and its homologues, p63 and p73, induce a replicative senescence through inactivation of NF-Y transcription factor. Oncogene. 2001; 20:5818–5825. [PubMed: 11593387]
56. Qian Y, Chen X. Senescence regulation by the p53 protein family. Methods Mol. Biol. 2013; 965:37–61. [PubMed: 23296650]
57. Chatelut E, Delord JP, Canal P. Toxicity patterns of cytotoxic drugs. Invest. New Drugs. 2003; 21:141–148. [PubMed: 12889735]
58. Widakowich C, de Castro G Jr, de Azambuja E, Dinh P, Awada A. Review: side effects of approved molecular targeted therapies in solid cancers. Oncologist. 2007; 12:1443–1455. [PubMed: 18165622]
59. Fujiwara T, Grimm EA, Mukhopadhyay T, Zhang WW, Owen-Schaub LB, Roth JA. Induction of chemosensitivity in human lung cancer cells in vivo by adenovirus-mediated transfer of the wild-type p53 gene. Cancer Res. 1994; 54:2287–2291. [PubMed: 8162565]
60. Forsythe JA, Jiang BH, Iyer NV, Agani F, Leung SW, Koos RD, Semenza GL. Activation of vascular endothelial growth factor gene transcription by hypoxia-inducible factor 1. Mol. Cell Biol. 1996; 16:4604–4613. [PubMed: 8756616]
61. Teodoro, JG., Evans, SK., Green, MR. J. Mol. Med. Vol. 85. Berlin: 2007. Inhibition of tumor angiogenesis by p53: a new role for the guardian of the genome; p. 1175-1186.
62. Ren B, Yee KO, Lawler J, Khosravi-Far R. Regulation of tumor angiogenesis by thrombospondin-1. Biochim. Biophys. Acta. 2006; 1765:178–188. [PubMed: 16406676]
63. Salimath B, Marme D, Finkenzeller G. Expression of the vascular endothelial growth factor gene is inhibited by p73. Oncogene. 2000; 19:3470–3476. [PubMed: 10918605]
64. Vikhanskaya F, Bani MR, Borsotti P, Ghilardi C, Ceruti R, Ghisleni G, Marabese M, Giavazzi R, Broggini M, Taraboletti G. P73 Overexpression increases VEGF and reduces thrombospondin-1 production: implications for tumor angiogenesis. Oncogene. 2001; 20:7293–7300. [PubMed: 11704858]
65. Ji W, Zhang W, Xiao W. E2F–1 directly regulates thrombospondin 1 expression. PLoS One. 2010; 5:e13442. [PubMed: 20976175]

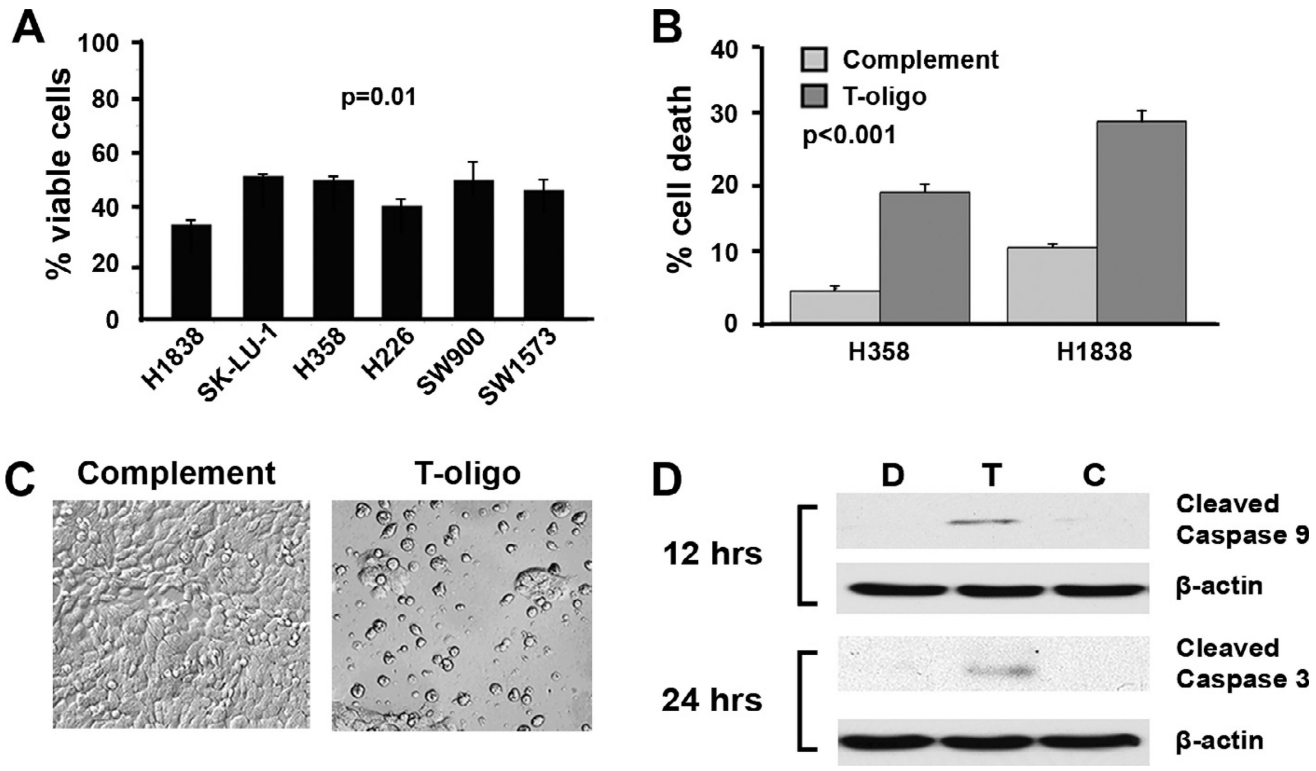

Fig. 1.

Treatment with T-oligo decreases NSCLC cell proliferation and induces cell death. H1838, SK-LU-1 H358, H226, SW900, SW1573 NSCLC cells were treated with 40 μM T-oligo, complementary oligonucleotide, or diluent for 96 h and then evaluated for cellular proliferation after trypan blue exclusion. (A) All NSCLC cell lines exhibited a 40–50% decrease in the number of viable cells after treatment with T-oligo. (B) A 3-fold increase in cell death was seen in H1838 and 4-fold increase in H358 cells treated with Toligo for 96 h after staining with propidium iodide and analyses by FACS scan of cells using sub G_0/G_1 DNA compared to complementary oligonucleotide treated cells. Results are from representative experiments with a significance of $p < 0.001$. (C) Images of H1838 cells treated with either T-oligo or complementary oligonucleotide show a decrease in cell survival after treatment with T-oligo for 96 h. (D) Activation of caspase 9 (20-fold increase) and 3 (4-fold increase) were seen in H1838 cells at 12 and 24 h, respectively, indicating that activation of a pro-apoptotic cascade had occurred in these cells.

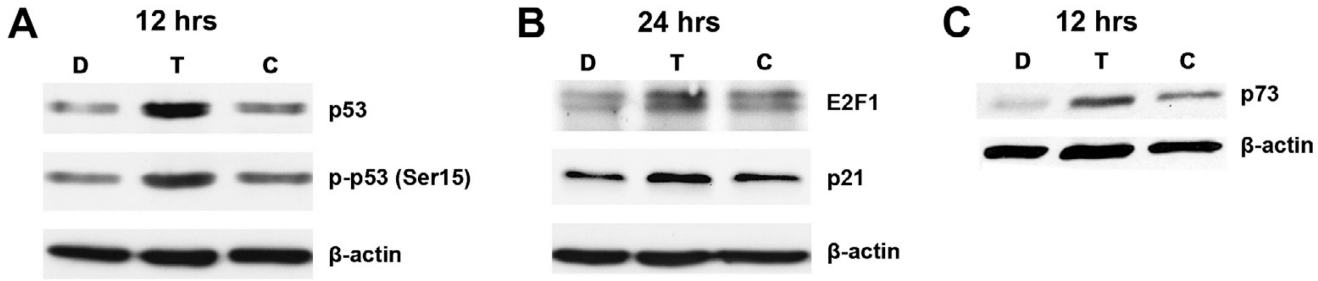

Fig. 2.

T-oligo induces expression of p53 and its homologue, p73. SW1573 and H358 cell lysates were prepared 12 and 24 h after exposure to 40 μM T-oligo, and subsequently immunoblotted. (A) SW1573 cells treated with T-oligo exhibited upregulation of p53 (2.5-fold increase) and activated phospho-p53 (Ser-15) (2-fold increase) at 12 h. (B) Upregulation of p21 (1.5-fold increase) was seen at 24 h in addition to an upregulation of E2F1 in SW1573 cells (2-fold increase). (C) H358 cells which have a homozygous deletion of p53, exhibit upregulation of p73 (2.5-fold increase), a p53 homologue 12 h after treatment with T-oligo.

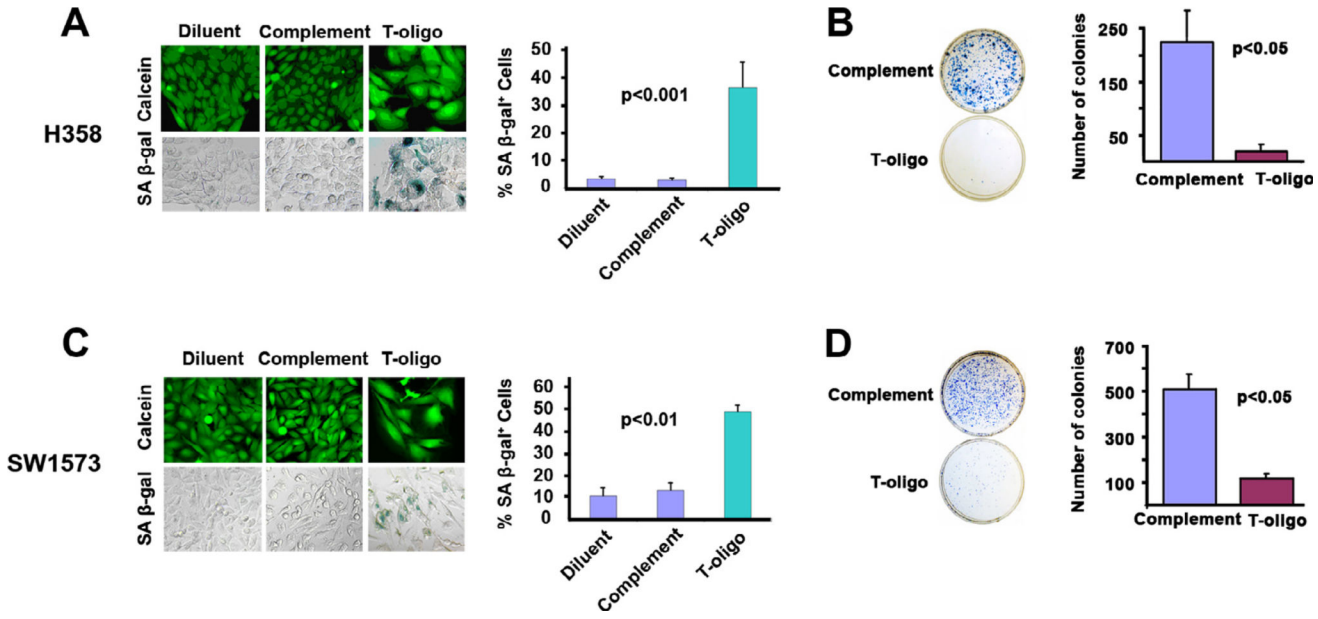

Fig. 3.

Exposure to T-oligo induces senescence in NSCLC cells. H358 and SW1573 cells were treated for one week with 40 μM of T-oligo, complementary oligo, or diluent and evaluated for a senescence-associated phenotype including morphology changes, positive staining for β-Galactosidase, and reduced clonogenicity. (A) H358 lung cancer cells treated for one week with T-oligo show a 12-fold increase in staining for senescence associated β-Galactosidase which appears as blue–green color. H358 cells treated with Toligo also exhibit a senescent morphology including an increased size similar to senescent fibroblasts as seen with Calcien AM staining. No senescence-associated changes were observed with complementary oligo or diluent controls. (B) Clonogenicity, a marker of senescence, was determined in H358 cells by treating cells for one week with complementary oligonucleotide or T-oligo and subsequently plating 2000 cells/well, culturing for eight days and then staining cells with 1% methylene blue in PBS. T-oligo decreased clonogenicity of H358 cells by 12-fold as compared to control. (C) SW1573 lung cancer cells treated with T-oligo for one week exhibited a 4-fold increase in positive staining for senescence associated β-Galactosidase, and on staining with Calcein AM, cells show an enlarged cell body. Minimal senescence associated changes were observed with complementary oligo or diluent controls. (D) Treatment of SW1573 cells with T-oligo reduced clonogenicity by 4-fold as compared to complementary oligonucleotide. (For interpretation of the references to colour in this figure legend, the reader is referred to the web version of this article.)

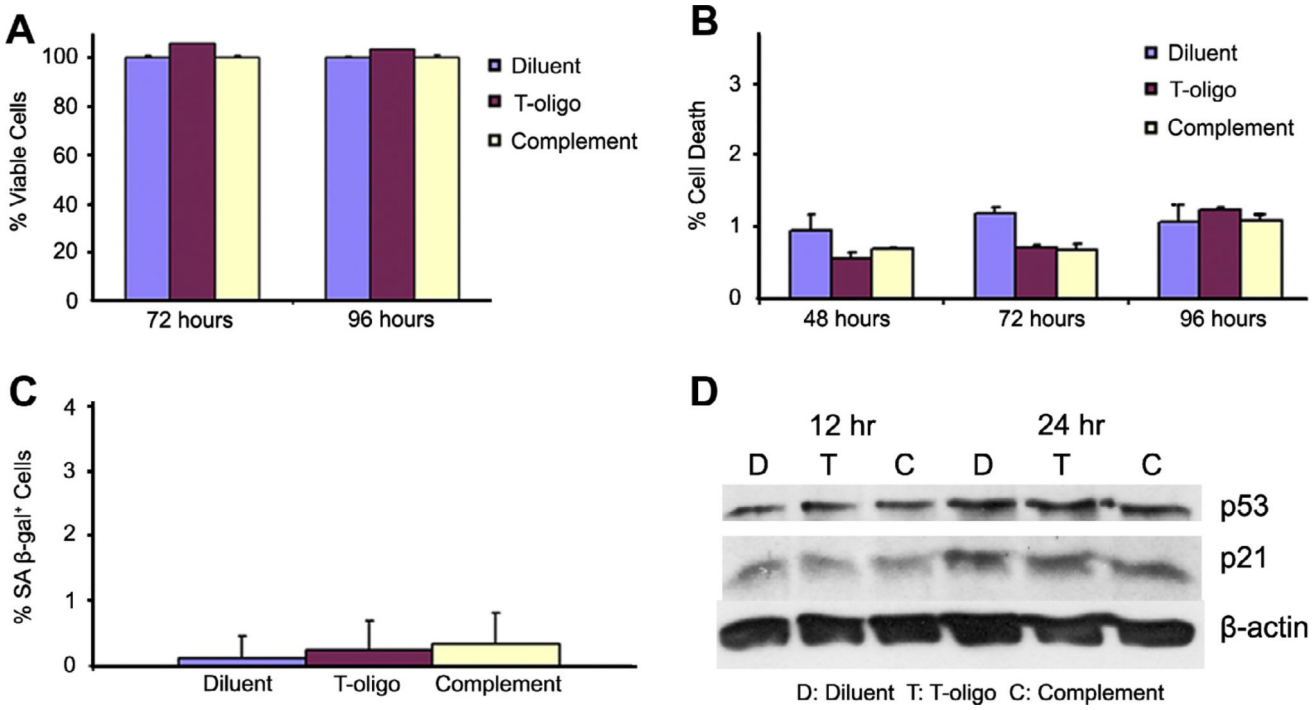

Fig. 4.

T-oligo has no affect on NBEC. NBEC were plated and treated with diluent, T-oligo, or complementary oligo for 12, 24, 48, 72, or 96 h and evaluated for proliferation, cell death and protein expression. (A) T-oligo did not inhibit proliferation in NBEC at 72 and 96 h as determined by viability cell counting by trypan blue exclusion. (B) Cells were collected at 72 and 96 h after treatment and subsequently fixed and stained with propidium iodide. FACS analysis of cells for sub G_0/G_1 DNA demonstrated that T-oligo did not induce cell death in NBEC. (C) Cells were treated with diluent, T-oligo or complementary oligo for one week and stained for the presence of senescence associated β-Galactosidase. It was found that T-oligo does not induce expression of senescence associated β-Galactosidase in NBEC. (D) NBEC lysates immunoblotted for p53 and p21 did not show an increase in either p53 or p21 in response to treatment with T-oligo, unlike results seen previously in SW1573 cells.

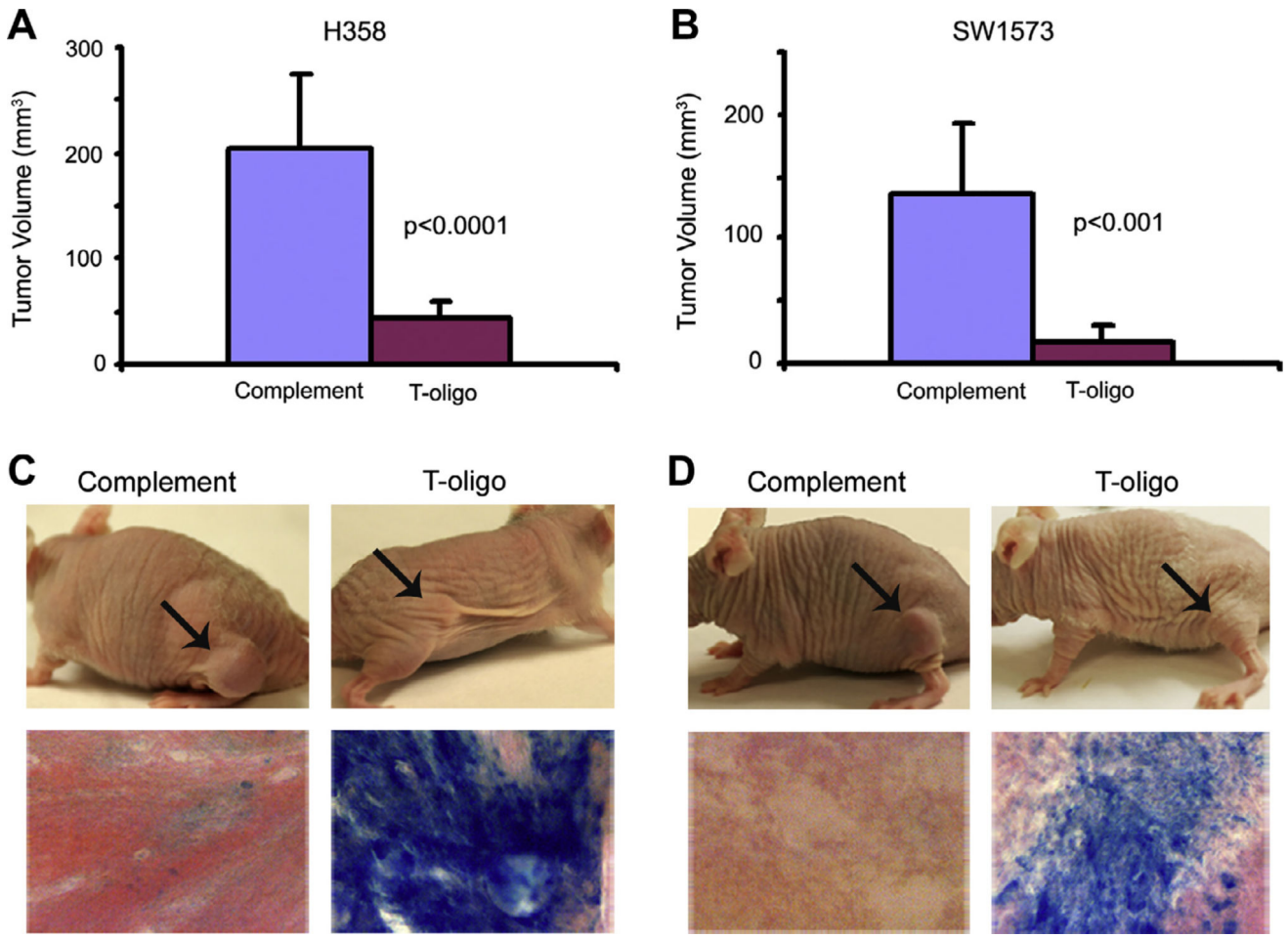

Fig. 5.

H358 and SW1573 lung cancer cells (5×10^6) were injected subcutaneously into the flank of nude mice. Tumors were allowed to grow for one week and then treated daily with T-oligo or complementary oligo in PBS for seven weeks. (A) T-oligo reduced tumor volume by 4.3-fold in H358 as compared to complementary oligo. (B) T-oligo reduced tumor volume by 5.6-fold in SW1573 tumors as compared to complementary oligo. (C,D). Both H358 and SW1573 tumors treated with T-oligo showed markedly reduced tumor volume and significant increase in expression of senescence-associated β-Galactosidase staining.

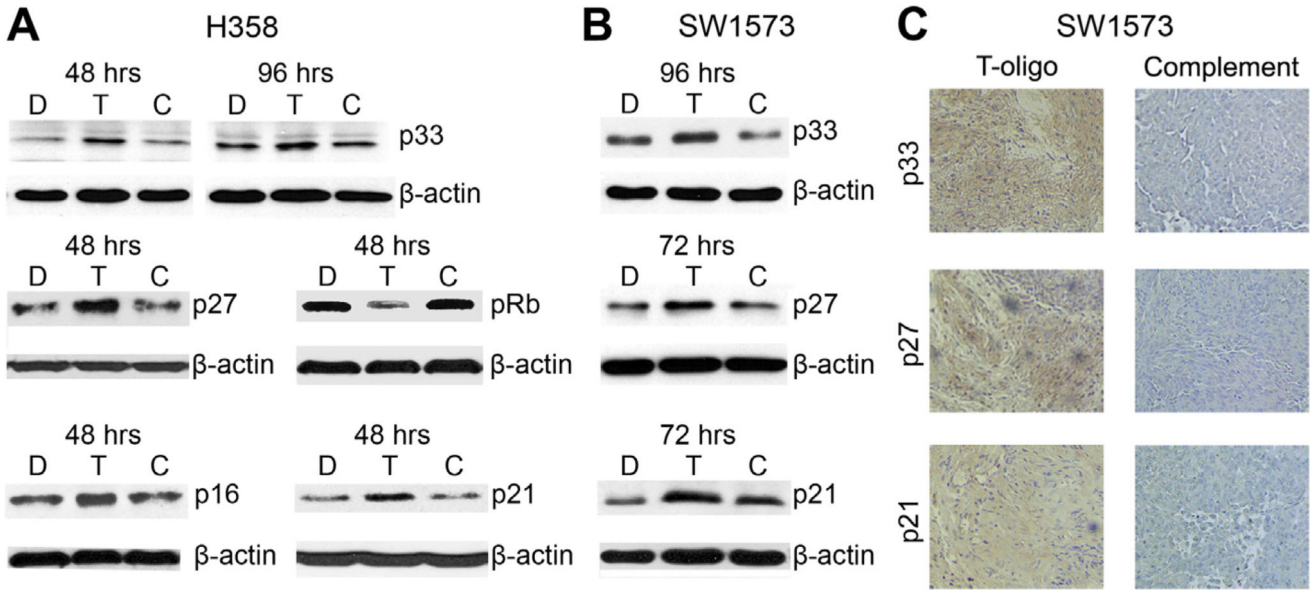

Fig. 6.

T-oligo induces senescence *in vivo* and *in vitro* through p33, $p27^{kip1}$, pRb, p16 and p21. H358 and SW1573 NSCLC cell lysates and tumor sections were evaluated for a change in expression of senescence inducing proteins by immunoblotting. (A) Treatment with T-oligo *in vitro* increased the expression of p33 at 48 (2.2-fold) and 96 h (1.6-fold) in H358 cells and increased the expression of $p27^{kip1}$ (1.8-fold), pRb (3-fold), p16 (2-fold) and p21 (2-fold) at 48 h. (B) T-oligo induced an upregulation in p33 expression *in vitro* in SW1573 cells at 96 h (2-fold), and an increase in expression of both $p27^{kip1}$ (1.8-fold), and p21 at 72 h (2-fold). (C) Paraffin sections of SW1573 tumors were stained using the M.O.M. kit (Vector) with antibodies against p21, $p27^{kip1}$, and p33. Tumor sections treated with complementary oligonucleotide showed no significant expression of p21, $p27^{kip1}$ or p33, while tumors treated with T-oligo show marked increase in expression of p21, $p27^{kip1}$, and p33 as indicated by the light brown staining.

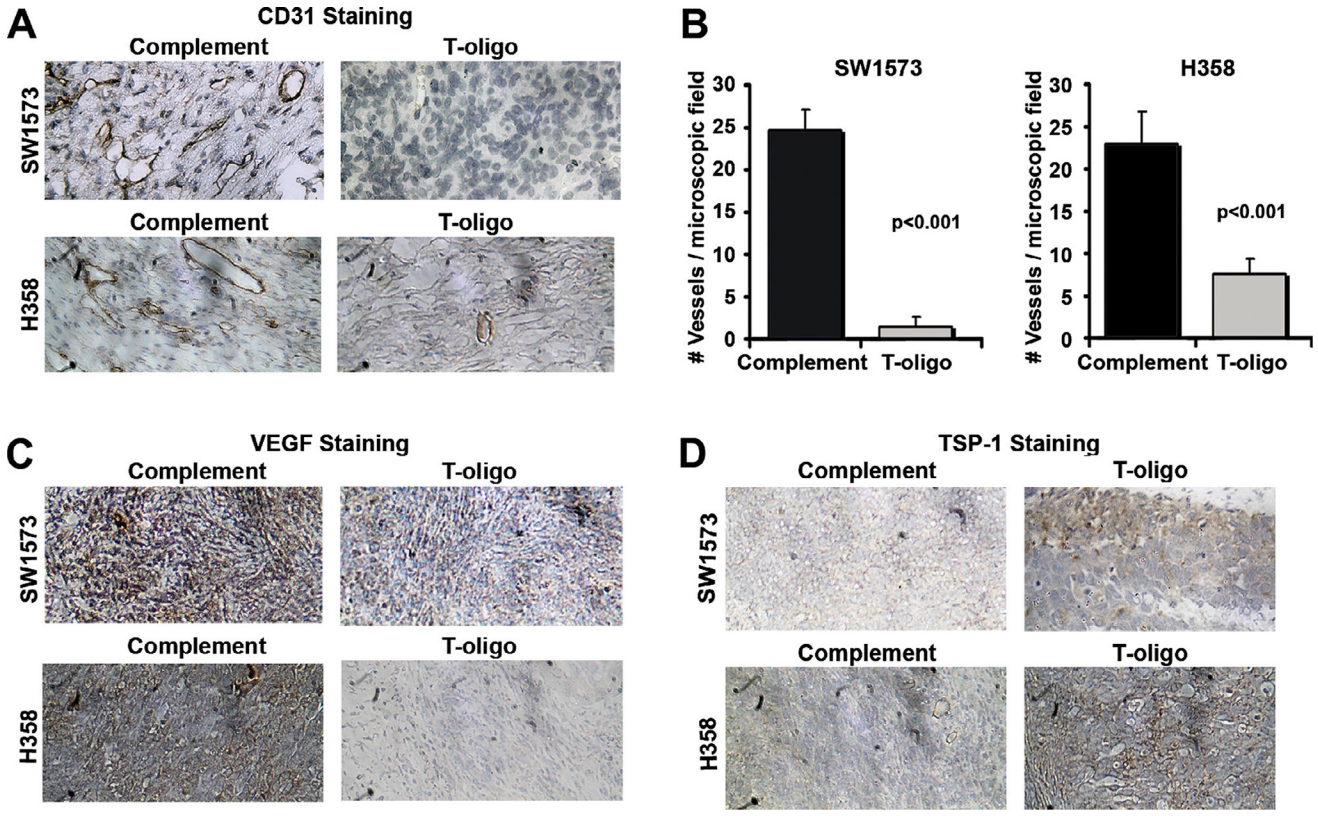

Fig. 7.

NSCLC angiogenesis is inhibited by exposure to T-oligo. H358 and SW1573 tumor sections were evaluated by IHC for evidence of angiogenesis. (A) H358 and SW1573 tumors were analyzed for vessel density by staining for the presence of the endothelium specific marker, CD31. A significant decrease in vessel density was observed in both H358 and SW1573 tumors treated with T-oligo. (B) A decrease in vessel density was further validated by totaling the number of intact vessels in 10 microscopic fields. T-oligo treatment decreased total vessel number by 2.2- and 3-fold in H358 and SW1573, respectively. (C) Tumor sections were also stained for the presence of VEGF, which is markedly decreased in T-oligo treated tumors as compared to complimentary oligonucleotide. (D) Additionally, H358 and SW1573 tumors immunostained for TSP-1, a potent inhibitor of angiogenesis, demonstrate a marked increased in TSP-1 after exposure to T-oligo.